Quantum size effects in metal films: Energies and charge densities of Pb(111) grown on Cu(111)

Giuliana Materzanini,[1,2] Peter Saalfrank,[2,3] and Philip J. D. Lindan[4,5]
[1]*Università degli Studi di Milano, Dipartimento di Chimica Fisica ed Elettrochimica, Via Golgi 19, 20133 Milano, Italy*
[2]*University College London, Chemistry Department and Centre for Theoretical and Computational Chemistry (CTCC), 20 Gordon Street, London WC1H OAJ, United Kingdom*
[3]*Universität Regensburg, Institut für Physikalische und Theoretische Chemie, D-93040 Regensburg, Germany*
[4]*Physics Laboratory, School of Physical Sciences, University of Kent at Canterbury, Canterbury CT2 7NR, United Kingdom*
[5]*Formerly at CLRC Daresbury Laboratory, Warrington WA4 4AD, United Kingdom*
(Received 12 June 2000; published 18 May 2001)

Energies and electron densities of free-standing Pb(111) slabs consisting of 1 to 15 layers have been determined by means of *ab initio* total energy calculations, using periodic slab geometries and gradient-corrected density functional theory. Two sets of calculations were carried out, one with fixed slab geometries and another one where interlayer spacings were fully relaxed. We find quantum size effects (QSE's) for the total energies in agreement with experiments by Toennies *et al.* [Europhys. Lett. **10**, 341 (1989)], who monitored the epitaxial growth of thin Pb films on a Cu(111) substrate. QSE's are also observed for the surface electron density of thin lead films which manifest themselves as different ''apparent step heights'' of the individual layers in high resolution helium atom scattering [Surf. Sci. **384**, L858 (1997)]. For this second QSE, we find that the interplane relaxation but also the in-plane strain within the Pb layers imposed by the Cu(111) substrate, are important factors when it comes to a quantitative comparison between theory and experiment.

DOI: 10.1103/PhysRevB.63.235405 PACS number(s): 68.35.Bs, 71.15.Mb

I. INTRODUCTION

Electron confinement causes quantization, and hence new, fundamentally interesting and possibly technologically relevant phenomena. A good example is the occurrence of so-called quantum size effects (QSE's) (Ref. 1) in thin metal films, where conduction electrons move quasifreely in the lateral (x,y) directions, while their motion perpendicular to the film surface (z), is quantized in a particle-in-a-box-like fashion. Many other nanostructured systems are known to exhibit QSE, ranging from ''zero-dimensional'' free[2] and deposited clusters and islands,[3] over fractal aggregates[4] and quasi-one-dimensional, chainlike structures,[5] to two-dimensional arrangements such as semiconductor[6] or metal films.

While QSE's have long been known to exist in semiconductors,[6] their occurrence in metallic, quasi-two-dimensional structures has been established only more recently. On the basis of self-consistent jellium calculations, Schulte[7] predicted that a number of electronic properties would exhibit oscillations as a function of the metal film thickness D due to QSE's. These properties include, among others, (1) the total energy, (2) the electron density inside and outside the film, (3) the density of states at various energies, and (4) the work function. Several theoretical studies asserted that characteristic oscillations should also exist for ''real'' metal films, when treated by more sophisticated first-principles electronic structure methods.[8–11] Examples have been reported for Al,[8,9] Li,[10] Rh,[8] and Pb films.[11]

Experimentally, QSE's were first seen for metals in the pioneering work of Jacklevic *et al.* who measured tunnelling currents in metal-metal oxide-metal junctions,[12] and later in low-energy electron transmission experiments by Jonker *et al.*[13] Since then, QSE-related oscillations have been found in other transport properties of thin films, such as the electric resistivity,[14] the Hall coefficient,[15] and the critical temperature in superconducting films[16] all of which depend all on the density of states at the Fermi energy. To our knowledge, no clear direct experimental evidence exists so far for QSE-type oscillations in the work function of metallic films. Moreover, the recently discovered oscillatory interlayer coupling between two ferromagnetic layers separated by a nonmagnetic spacer[17] has been found to be closely related to the appearance of quantum well states at the Fermi level in the spacer thin metal film.[18] These experimental findings inspired a great amount of theoretical work, and *ab initio* calculations have been performed which confirmed the experimental long and short range periods of the oscillations.[19] Novel applications of these QSE's such as giant magnetoresistance and tailoring of magnetic sensors and spin valves, are nowadays the subject of a number of first-principles studies.[20,21]

In this paper we study oscillations in the energies and the electron densities of thin nonmagnetic metal films. To this end first-principles slab calculations using gradient-corrected density functional theory (DFT) have been carried out for the example of Pb(111) films consisting of 1 to 15 monolayers (ML's). Oscillations in the total energy are expected to influence the growth mechanism of a film, while differences in the electron densities—in particular in the ''vacuum'' region, i.e., outside the metal—should, indirectly, determine the work function and hence, for example, the reactivity or the spectroscopical properties of the system.

The motivation to study lead films comes from two key experiments by Toennies and co-workers. The first one revealed, by helium atom scattering (HAS), oscillatory behavior in the total energies with the number of Pb monolayers during the epitaxial film growth on a Cu(111) substrate.[22] In particular, regions were identified where a double-layer growth pattern dominated over a layer-by-layer mode, suggesting that ''magic numbers'' exist for extended film struc-

tures, as well as for (metal) clusters.[2] In the second, more recent experiment HAS was used in an interferometric mode to measure the ''apparent step height'' of Pb layers grown on Cu(111).[23] Roughly speaking, in this experiment one probes regions of constant electron density above the film, and therefore the extent of the ''spill-out'' of the electrons into the vacuum. Again, characteristic oscillations were found with a double-layer period, which show that the electron density outside the film is influenced by QSE's, as predicted by Schulte.[7] Toennies and co-workers rationalized their findings in both experiments nicely with the help of particle-in-a-box–type models. The major aim of the present contribution is to provide a more solid theoretical understanding of the underlying physics, which also accounts for the ''real'' electronic and geometric structure of thin Pb films. To this end *ab initio* electronic structure theory is applied, supported by more simple concepts.

The rest of the paper is organized as follows. In Sec. II the methodology of the present calculations is outlined, together with a few specific numerical details. In Sec. III, *n*-layer Pb films ($n=1-15$) are studied to rationalize oscillations in the total energies. The role of interplane relaxation of the Pb ion cores is investigated by comparing the results of calculations with and without structural relaxation. We observe trends that are consistent with the growth mechanism of lead films on Cu(111) suggested in Ref. 22. The computed interlayer distances for the optimised geometries are compared to experiment.[24] In Sec. IV the *ab initio* based method used to compute the apparent step heights is outlined, and the results are presented and related to experiment.[23] It turns out that not only the interplane relaxations but also the inclusion of intraplane strain imposed by the Cu(111) substrate is an important factor when it comes to a quantitative comparison to the HAS data.[23] Finally, Sec. V contains a summary of the work and our conclusions.

II. METHOD

A. Generalities

For performing ground-state electronic structure calculations on the Pb(111) slabs within the DFT formalism, we have used the Cambridge Serial Total Energy Package (CASTEP), employing a supercell geometry.[25] The program solves the periodic Kohn-Sham equations of density functional theory (DFT).[26] For all calculations the generalized-gradient approximation (GGA) was used in the form given by Perdew and Wang.[27] For the $14\,5d$, $6s$, $6p$ Pb valence electrons a plane-wave basis set is used, the size of which is determined by an energy cutoff E_c and the volume of the unit cell.[25] The ionic cores of the Pb atoms are represented by fully separable, ultrasoft[28] pseudopotentials. A scalar-relativistic treatment has been chosen in which the mass velocity and the Darwin terms are retained in the full-core potential, while neglecting the spin-orbit correction[29] of the fully relativistic pseudopotential.[30] As will be argued later, this single-component approach does not affect any of our conclusions significantly.

Further, conjugate gradient and density mixing schemes[25,32] are used for iteratively minimizing the total energy functional in the space of the plane-wave expansion coefficients. Geometry optimization is achieved *via* a BFGS minimizer.[33] Finally, since we are dealing with metallic systems, we take advantage of the improved convergence yielded by smearing the occupation of the bands around E_F by a finite-T Fermi function and extrapolating to $T=0$ K.[34,31]

B. Specifics for Pb films

The initial convergence tests to determine suitable computational parameters were done for bulk Pb. For the primitive unit cell (1 Pb per layer), with a $5\times5\times5$ **k**-point mesh which corresponds to 10 **k** points in the irreducible part of the Brillouin zone (IBZ) according to the Monkhorst-Pack algorithm,[35] and with a plane-wave energy cutoff of $E_c=320$ eV the experimental lattice constant of $a_{\mathrm{exp}}=4.95$ Å (Ref. 36) could be reproduced to within 2% ($a_{\mathrm{the}}=5.02$ Å). The use of larger cutoff energies or **k**-point meshes did not alter this value significantly. A Fermi broadening of 0.2 eV was chosen to smear out the Fermi surface according to the finite-T scheme mentioned above. Total electronic energies were converged to within $\leqslant 2\times10^{-7}$ eV/atom.

The convergence also of other computed properties was checked carefully. For the QSE to be studied below an accurate determination of the Fermi surface and the band structure around E_F is crucial. Increasing the **k**-point mesh to $7\times7\times7$ (20 **k** points in the IBZ) did not alter the computed band structure for bulk lead significantly—the bands around E_F were typically shifted by $\approx$0.1 eV to lower energies, without notable influence on their shapes and widths. Also, spin-orbit corrections play only a minor role for the band structure around E_F. This conclusion was drawn from comparing our scalar-relativistic calculations for bulk Pb to an older DFT calculation[37] in which spin-orbit coupling had been included. Our Fermi surface was in quantitative agreement with the spin-orbit corrected one by Horn *et al.*[37] In particular, the numbers and positions of those points along high-symmetry lines in the IBZ that arise from the crossing of bands with E_F, were in excellent agreement. For example, there are two bands which cross E_F along the ΓK line at $|\mathbf{k}|=0.52$ and $0.71|\mathbf{k}_K-\mathbf{k}_\Gamma|$ according to Ref. 37, whereas we find two points at 0.55 and $0.72|\mathbf{k}_K-\mathbf{k}_\Gamma|$, respectively. For bulk Pb the Fermi surface arises from the two lowest $6p$ levels, whereas the $6s$ band is located between about 11.5 and 6.9 eV below E_F. Band widths in the Fermi region as well as s-p band gaps at various **k** points are in good agreement with Ref. 37, typically to within a few tenths of eV. (Remaining differences are mainly due to the use of different functionals in both works.) Significant differences due to spin-orbit coupling are found almost exclusively for bands well above E_F. An exception to the rule is a spin-orbit splitting of about 1.5 eV observed in Ref. 37 for the two lower p levels at point W of the IBZ which are situated close to E_F; this splitting is not recovered in our calculations. In general, however, the electronic states around E_F are largely unaffected by spin-orbit effects, and we expect the same for the QSE's to be studied below.

For the film calculations below, free-standing Pb films in periodic slab geometries were employed; the presence of a Cu(111) substrate was treated indirectly (see below). For a film consisting of n Pb monolayers, the unit cell contains n atoms. A $5\times5\times1$ k-point mesh was used, corresponding to 5 **k** points in the irreducible Brillouin zone, together with the cutoff energy determined for the bulk. The convergence criteria were 5×10^{-6} eV/atom for the electronic energy, and r.m.s. atom displacements less than 0.01 Å and forces less than 0.05 eV/Å for the geometry optimization. Unless stated otherwise, a vacuum gap of 13 Å was employed. This gap was sufficient to yield energies converged to within 1×10^{-2} eV per layer. More importantly, the electron density tails in the vacuum region are very sensitive to the vacuum gap between slabs. This in turn makes the calculation of the apparent step heights (see below) sensitive to the choice of vacuum gap. The value of 13 Å is sufficient for these purposes.

The slab calculations have been carried out with and without geometric relaxation of the ion cores. Relaxation amounts to optimizing the interlayer distances within a cell of fixed volume, since the shortest Pb-Pb distance within a layer is fixed by virtue of the periodic boundary conditions. This latter distance was $a_{\rm the}\sqrt{2}/2=3.55$ Å, slightly larger than the experimental value of 3.50 Å. In the unrelaxed calculations the intraplane distance was also fixed at the theoretical bulk value $d_0=a_{\rm the}/\sqrt{3}=2.90$ Å. Finally, to include the strain imposed on the Pb films by the rigid Cu(111) substrate in an approximate way, calculations with in-plane compression were carried out (see Sec. IV C for details).

III. ENERGETICS OF THIN Pb FILMS

The first part of this work aims at an understanding of QSE's previously detected during the growth of Pb overlayers on a Cu(111) substrate.[22] Total energy calculations of the type described above were carried out on Pb slabs with (111) surfaces, ranging from 1 to 15 layers thick.

A. Total energies and energy differences

In Fig. 1(a) we show the total energy per monolayer (i.e., per atom) $E(n)/n$ as a function of the number of layers in the slab n both for the unrelaxed and the relaxed geometries. It is seen that $E(n)/n$ is more negative at larger n, with only little structure in the curve. For larger n, $E(n)/n$ gradually approaches a constant value which in the limit is equal to the energy per atom in the bulk. Note that geometry optimization lowers the total energies, as expected, but the overall effect of interplane relaxation on the total energy trend is small.

A quantity which is much more sensitive to QSE's is the energy difference

$$\Delta E(n)=E(n)-E(n-1) \tag{1}$$

which is shown in Fig. 1(b). Now, clear oscillations which are ''damped'' at higher n become visible, both for the unrelaxed and the relaxed geometries. These oscillations arise from the occupation of electronic levels close to Fermi surface (see Ref. 7), which are p-like as for the bulk (see Sec. II B). Closer inspection shows that from $n=1$ to $n=6$ three oscillations with a double-layer period are present (''region A''), and similar oscillations occur between $n=10$ and $n=14$ (''region C''). Between $n=7$ and $n=9$ the oscillations are basically absent (''region B''). As we have carefully checked the convergence of the total energies and of the single-particle energies at the Fermi level over the k-point sampling (see Sec. II B), these changes in the oscillation periods cannot be due to numerical inaccuracies. Conversely, the oscillations in region A suggest that there films with an even number of monolayers (2,4,6), are more stable than those with an odd number (1,3,5), whereas in region C the odd-layer slabs (11,13,15) are energetically favored over the even ones (10,12,14). This suggests further that in regions A and C double-layer growth should prevail to maximise stability, whereas in region B monolayer-by-monolayer should dominate. In fact, Toennies *et al.* have observed precisely this kind of behavior for Pb growing on Cu(111), i.e., for up to $n\sim25$ there are regions dominated by a double-layer periodicity with monolayer-by-monolayer regions between them. The oscillations are damped at larger n, which is consistent with Fig. 1, and they are completely absent when Pb is deposited on Pb(111) where exclusively monolayer-by-monolayer growth takes place.[22]

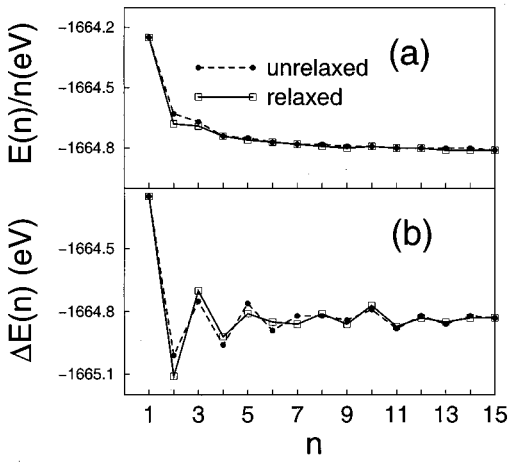

FIG. 1. (a) Monolayer energies $E(n)/n$ for relaxed and unrelaxed Pb(111) slabs as a function of the number of monolayers n; (b) corresponding energy differences $\Delta E(n)$ [Eq. (1)].

From a theoretical viewpoint, QSE in the total energies are not new, not even for Pb(111). They have been found (for $n\leqslant7$) by means of periodic Hartree-Fock calculations.[11] In more simple but insightful terms the oscillations arise, according to Schulte,[7] because the quantized one-electron energies decrease with increasing film thickness: then, every time such a level falls below the Fermi energy E_F it becomes filled suddenly thus leading to a discontinuous energy jump. In a simple particle-in-a-box type picture, the one-electron energy levels are[7]

$$\varepsilon_j(k_x,k_y)=\frac{\hbar^2(k_x^2+k_y)^2}{2m}+\frac{\hbar^2\pi^2j^2}{2mD^2}+v_0, \tag{2}$$

where m is the electron mass (assumed to be isotropic), $\hbar k_x$ and $\hbar k_y$ are the electron momenta for free motion along x

and y, D is the box width, taken to be equal to the film thickness, $j>0$ is a quantum number, and v_0 a constant. Equation (2) clearly reflects how the energy levels are stabilized with increasing film thickness.

Another equally intuitive and simple viewpoint was suggested in Ref. 22 where it was argued that the oscillations can also be explained with the magnitude of the so-called misfit, defined as

$$\delta(n)=\left| nd_0 - m\frac{\lambda_F}{2}\right|. \tag{3}$$

(n is the number of layers, d_0 the distance between two layers, λ_F is the Fermi wave length, and m an integer which makes δ a minimum). The confining potential of the film is modelled by a box of width $D=nd_0$. Whenever δ is large the standing electron waves do not fit properly into this box, and the film is less stable. The misfit $\delta(n)$ as a function of n will be shown below; for now it is sufficient to say that according to Toennies, $\delta(n)$ correlates nicely with the observed growth pattern monitored with HAS.[23]

B. Interplane relaxation

Although the occurrence of QSE-related oscillations in the energies does not depend on interplane relaxation, the latter is substantial, and does influence the apparent step heights to be calculated below. It is therefore worthwhile to discuss the effects of geometry relaxation a little further and to judge on the quality of our calculations by comparing to experiment. Let us define

$$\delta_{ml}(n)=[Z_l(n)-Z_m(n)-(l-m)d_0]/d_0\times 100\% \tag{4}$$

as the percentage measure for the geometric relaxation of the distance between the lth and the mth layers within an n-layer film. The convention used is that the outermost layer is the first one. Here, $Z_l(n)$ is the position along z of the ions in layer l, and $Z_l(n)-Z_m(n)$ is the optimized distance between the two layers while $(l-m)\times d_0$ is the corresponding distance in the unrelaxed case. Since the geometric relaxation is in general different for different slab thicknesses n, δ_{ml} depends on n. In Fig. 2 we show δ_{12} (a), δ_{23} (b), and δ_{34} (c), as a function of n.

By considering Fig. 2(a) we find that δ_{12} is (i) negative and (ii) oscillates, approaching a final value of about -5%. The first observation means that the distance between the top and the second layer is smaller than in the bulk, a well-known and well-understood effect for many surfaces.[38,24] The oscillations reflect QSE in Pb layers, and in fact they have their consequences when the quantitative determination of apparent step heights in HAS is of concern. After 15 ML the oscillations are still visible which indicates that the semi-infinite surface limit is still not reached. The distance between the top and the first subsurface layer of a Pb(111) surface as determined by LEED is $-3.5\pm 1.0\%$,[24] which is in fair agreement with the theoretical value for $n=15$.

Figure 2(b) shows (except for $n=5$) positive values for δ_{23}, indicating that the distance between the second and third layer is somewhat widened. The geometry change is

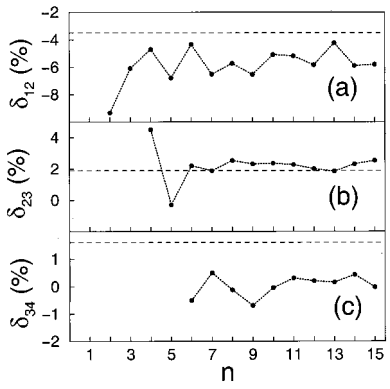

FIG. 2. Percentage interlayer relaxations δ_{lm} [Eq. (4)] for Pb(111), as a function of slab thickness n. Shown are the relaxations of the distance between the first (top) and second layer (a), the second and third layer (b), and the third and fourth layer (c). The dashed, horizontal lines are the experimental values for a semi-infinite Pb(111) surface (Ref. 24).

less pronounced than for the (1, 2) pair as might be expected, and the $n=15$ value of δ_{23} is $+2.4\%$ and thus in good agreement with experiment, which gives $+1.9\pm 1.4\%$.[24] For the (3, 4) pair we find only a small relaxation parameter δ_{34}, whose sign depends on the layer thickness. The ''final'' δ_{34} (for $n=15$) of about $+0.5\%$ is smaller than the experimental value of $+1.6\pm 1.8\%$.[24] Taking the experimental error bars into account and the fact that a film is still different from a semi-infinite surface, the magnitude of the geometric relaxation is captured reasonably well by the calculations.

IV. CHARGE DENSITIES OF THIN Pb FILMS

A. Apparent step heights: How to calculate them

In this section we are concerned with the second key experimental finding mentioned above, namely the occurrence of oscillations of the apparent step heights of Pb films when grown on Cu(111), measured by interferometric HAS.[23] In these experiments every time a monolayer of lead was half-completed the growth process was halted, the energy of the helium beam was linearly increased from 12 to 80 meV and a time-of-flight spectrum was recorded, from which the heights of consecutive layers were obtained. The term ''apparent'' hints to the fact that not only the geometric distance between the ionic cores in complete and half-complete layers contribute to the step height, but also the electron density outside the layers does. If the He scattering process is treated classically, the apparent step height (ASH in the following), for a film consisting of $n-1$ complete and one incomplete layer is

$$d(n)=Z_1(n)-Z_1(n-1)+z_{tp}(n)-z_{tp}(n-1). \tag{5}$$

Here, $Z_1(n)$ $[Z_1(n-1)]$ is the geometric position of the ion cores in the uppermost layer 1 of an n $(n-1)$ layer system, while $z_{tp}(n)$ $[z_{tp}(n-1)]$ is the height above that layer that corresponds to the classical turning point of the He atom. The latter probes constant electron density of the film in the vacuum region as long as the kinetic energy of the He atom

is constant. In the range of He kinetic energies considered here the attractive well in the rare gas-film interaction can be neglected; then the He-surface interaction potential is repulsive and depends according to Esbjerg and Nørskov[39] linearly on the electron density spilling out into the vacuum:

$$V(z)=A\rho(z). \tag{6}$$

Here, $A=111.0$ when the interaction energy is measured in eV and the electron density $\rho(z)$ in electrons/Å^3.[39] At the classical turning point above an n-layer film, say, the kinetic energy of the projectile He atoms equals the repulsive interaction with the film

$$V[Z_1(n)+z_{tp}(n)]=E_k \tag{7}$$

such that z_{tp} can be extracted from E_k and the electron density $\rho(z)$. Hence, Eq. (5) suggests that the apparent step height has two contributions, namely, a *geometric* one [owing to the position of the ion cores $Z_1(n)-Z_1(n-1)$], and an *electronic* one [owing to the classical turning points $z_{tp}(n)-z_{tp}(n-1)$]. Both quantities depend on the number of layers n because the interlayer relaxation is different for different film thicknesses (see Fig. 2), but also the electron density profile extending from the surface into the vacuum depends on n (see below). Furthermore, the ASH will depend on the kinetic energy of the He atoms because z_{tp} will be smaller for higher initial E_k.

The dependence of the apparent step heights on E_k and the dependence of z_{tp} on n have been investigated in Ref. 23 using simple square-well model potentials and particle-in-a-box–type energies. These calculations rationalized the experimental findings, namely, distinct oscillations of the ASH with the number of Pb monolayers and a 2 ML period around d_0, which is again the geometric distance between two layers in the bulk. According to Ref. 23 these oscillations are due to different spill-outs of electron density into the vacuum, i.e., due to QSE-related differences in the electron density above the film as predicted by Schulte.[7] In the present work we will try to rationalize these findings on an *ab initio* basis, further discriminating between geometric and electronic contributions.

Again, as a first step free-standing Pb(111) slabs are considered and the Cu(111) substrate neglected. The calculation of the apparent step heights requires the knowledge of the ion core positions and of the electron density outside the film.

The relevant quantity here is the *laterally averaged* electron density $\overline{\rho}$, obtained from integrating over the area A_0 of the two-dimensional unit cell:

$$\overline{\rho_n}(z)=\frac{1}{A_0}\int\int \rho_n(x,y,z)dxdy. \tag{8}$$

In Fig. 3 we show $\overline{\rho_n}(z)$ for films consisting of $n=3$ [Fig. 3(a)] and $n=4$ layers [Fig. 3(b)], with and without geometry optimization. The HAS experiments of Toennies *et al.*[23] were carried out in a kinetic energy range between 12 and 80 meV, thus indicating via Eq. (6) that He is reflected from the film at electron densities ranging from 1.1×10^{-4} to

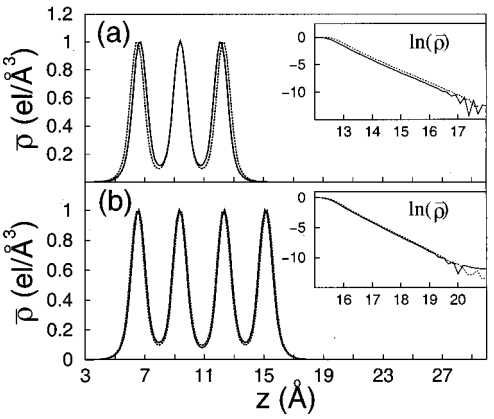

FIG. 3. Laterally averaged electron densities $\overline{\rho}(z)$ [Eq. (8)] for Pb(111) consisting of $n=3$ (a) and $n=4$ layers (b), respectively. Solid lines are for the relaxed films, dashed ones for unrelaxed slab geometries. The insets show $\ln(\overline{\rho})$ vs z in the vacuum region.

7.3×10^{-4} electrons/Å^3. Hence only the low-density tails in Fig. 3, far away from the film, are of interest when interpreting these experimental data.

As a ''reference density'' we will take $\overline{\rho}=1\times10^{-4}$electrons/Å^3. This is at the lower end of the He kinetic energies considered in Ref. 23, but test calculations showed that densities higher by a factor of 10 give still very similar results [see also Fig. 5(a) below]. Occasionally, however, lower densities will be considered. Note that it is difficult to calculate precise densities at low values. First, the vacuum gap has to be chosen large enough to avoid interference of the electron tails of neighboring slabs, and the numerical precision of the calculation must be high. Second, an accurate sampling of the Fermi surface in particular around Γ is required for the same reason—see Ref. 40 for the related problem of calculating matrix elements of STM currents. Finally, another problem arises from the fact that neither the LDA, nor the GGA functionals used here, give the correct asymptotic behavior, which here translates to large z. For atoms or molecules it is known that the correct asymptotic density is[41]

$$\lim_{r\to\infty}\rho(r)=Be^{-a\sqrt{I}r}, \tag{9}$$

where r is the distance from the atom (molecule), I is its ionization potential, and a and B are constants. We can impose the correct exponential asymptotics for our film problem, i.e., at large z, $\overline{\rho}(z)$ should fall off exponentially. The insets of Fig. 3, where $\ln[\overline{\rho}(z)]$ is shown as a function of z, suggest that indeed from about 1 Å above the surface the electron density falls off exponentially, i.e., $\ln[\overline{\rho}(z)]$ decreases linearly with increasing z. If the functional were ''exact,'' we could extract the work function from the slope, since according to Eq. (9) the exponent depends via a square-root law on the energy required to remove an electron. At distances larger than about 5 Å from the surface, artificial oscillations occur which are due to the finite vacuum gap and finite numerical precision. With our choice of a 13 Å gap we can see from Fig. 3 that electron densities down to $\sim1-2$

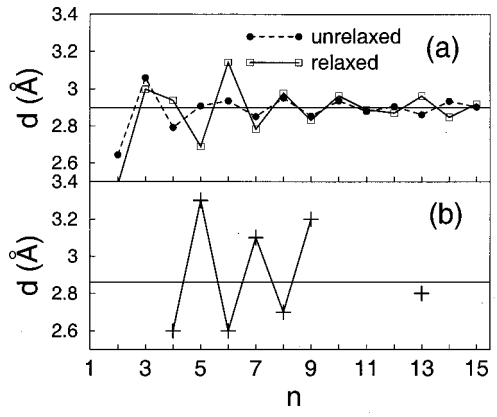

FIG. 4. Apparent step heights d: (a) calculated values for $\overline{\rho}=1\times10^{-4}$ electrons/Å^3; (b) experimental values from Ref. 23.

$\times10^{-5}$ electrons/Å^3 can be calculated without encountering these artificial structures. We have exploited the linear relation between $\ln[\overline{\rho}(z)]$ and z in the density interval between 10^{-2} and 10^{-3} electrons/Å^3 to extrapolate to lower electron densities. The vacuum gap used here leads to an uncertainty in the apparent step heights of around 10^{-2} Å for electron densities in the range between 10^{-2}–10^{-3} electrons/Å^3. There is still, however, an error due to the ''wrong'' density functional. In passing we note that the extrapolation procedure does not make superfluous the need for a large enough vacuum gap, because a gap too small renders the extrapolation inaccurate. In our case, gaps smaller than 13 Å caused problems.

B. Apparent step heights for lead films

Figure 4(a) shows calculated apparent step heights as a function of slab thickness for n ranging from 2 to 15. Values from both unrelaxed and relaxed calculations are shown. These are compared with experimental values in Fig. 4(b). The experimental data have been reported for up to $n=9$ only, with the exception of a single additional data point at $n=13$. For the calculations it was assumed that He atoms are elastically scattered as soon as the electron density reaches $\overline{\rho}=1\times10^{-4}$ electrons/Å^3. From the figure we can learn the following.

First, both in theory and in experiment oscillations of the apparent step height d around the ''expected step height'' d_0 are found. In particular, distinct areas with a clear 2 ML periodicity are visible. In both cases the oscillations appear to be damped for larger n. Hence, the DFT-slab calculations account for the major experimental findings, namely for QSE-related oscillations of the ASH of thin Pb(111) films.

Second, comparing the two theory curves it is obvious that relaxation is important. The unrelaxed slabs tend to diminish the amplitude of the oscillations, and they may even predict a different sign for $d-d_0$.

Third, by comparing theory and experiment more closely we note certain differences between the two. The theoretical, relaxed curve is shifted relative to the experimental one by one monolayer, e.g., $d(6,\text{experiment})-d_0<0$, $d(7,\text{experiment})-d_0>0$, while $d(6,\text{theory})-d_0>0$, $d(7,\text{theory})-d_0<0$. Also, at least for large n, the amplitude of the oscillations seems to be too small in the calculated values. We will address to these discrepancies shortly.

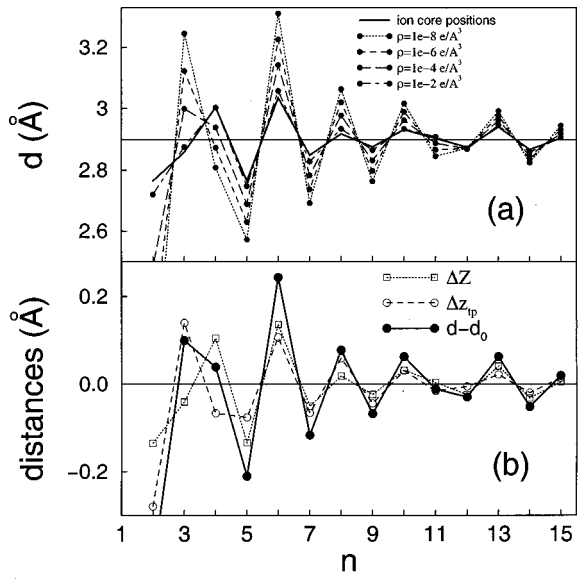

FIG. 5. (a) Apparent step heights for relaxed geometries, calculated at different values of the charge density $\overline{\rho}$, along with differences in the ionic core positions $Z_1(n)-Z_1(n-1)$; (b) the quantities $\Delta Z(n)$ [Eq. (10)] and $\Delta z_{tp}(n)$ [Eq. (11)], and their sum, $d-d_0$, for $\overline{\rho}=1\times10^{-4}$ electrons/Å^3.

As mentioned above the results shown in Fig. 4 are for a $5\times5\times1$ **k**-point mesh in the IBZ, including the Γ point. To address a possible sensitivity of the tails of the electron clouds in the vacuum region on **k**-point sampling, for $n=1$, 2, and 3 layers also test calculations with a $7\times7\times1$ mesh and, therefore, more accurate sampling around Γ were carried out. These resulted in changes of only $\Delta d(n)\sim0.002$ Å, indicating that also the electron spillout was converged with respect to **k**-point sampling.

We have computed the apparent step heights at a number of densities to investigate their dependence on the incident He-atom kinetic energy. These are shown in Fig. 5(a). (The range of densities corresponds to an incident kinetic energy range of 1.1×10^{-6} to 1.1 eV.) In this figure we also show $Z_1(n)-Z_1(n-1)$ to illustrate the relative importance of the electronic and geometric contributions to d. Several important points emerge from these results. We already know that unrelaxed structures exhibit QSE's in the apparent step heights, and therefore that the QSE's are in part related to the electronic structure changes as a function of n. Here though we see that the electronic and geometric contributions to d are of similar magnitude. We can also see that the amplitude of the QSE oscillations increases with decreasing E_k. Both the QSE's in the unrelaxed structures and the various theoretical models discussed earlier indicate that the density tails differ for different n. The change in amplitude of d with density (incident kinetic energy) is a direct consequence of this.

To further clarify the role of geometric and electronic effects, Fig. 5(b) shows

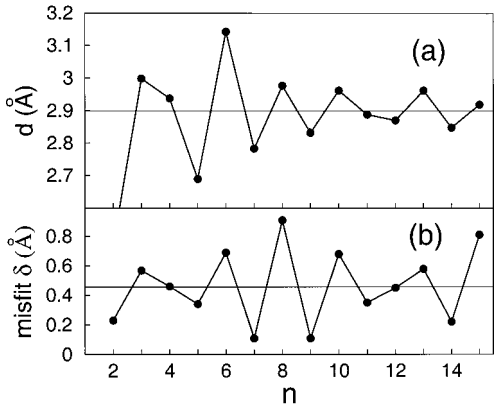

FIG. 6. (a) Calculated apparent step heights for relaxed geometries, $\overline{\rho}=1\times10^{-4}$ electrons/Å^3; (b) the ''misfit'' δ [Eq. (3)].

$$\Delta Z(n)=Z_1(n)-Z_1(n-1)-d_0 \tag{10}$$

and (for $\overline{\rho}=1\times10^{-4}$ electrons/Å^3)

$$\Delta z_{tp}(n)=z_{tp}(n)-z_{tp}(n-1). \tag{11}$$

These are measures of the change in apparent step height over and above that expected simply from the addition of an extra layer (i.e., d_0), due to geometric and electronic effects, respectively. The sum of these quantities, $\Delta Z+\Delta z_{tp}=d-d_0$, is also shown. If $\Delta Z+\Delta z_{tp}$ is >0, then the step appears higher than ''normal,'' and lower if $\Delta Z+\Delta z_{tp}<0$. It must also be emphasised that the electronic part Δz_{tp} is not independent of the geometric one, i.e., Δz_{tp} depends on whether the structure was optimized or not.

From Schulte's jellium calculations we know that in thin metallic films, due to the progressive falling of new electronic states below the Fermi energy during the film growth, not only the total energy differences but also the electron densities outside the surface oscillate as a function of film thickness. The same result is obtained from consideration of the misfit $\delta(n)$ defined in Eq. (3), which is a measure of how well a standing electron wave fits into a box of width D (see Sec. III). Every time δ is small the electrons are commensurate with the box and the electron density outside the film will be small. Hence, z_{tp} and the apparent step height will be small, because the He atoms can approach more closely. In contrast when δ is large, d is expected to be large. The proposed correlation between d and δ is impressively demonstrated in Fig. 6, where the geometry-optimized apparent step height for $\overline{\rho}=1\times10^{-4}$electrons/Å^3 [Fig. 6(a)], is compared with the calculated misfit δ for Pb(111) films consisting of n layers [Fig. 6(b)]. For δ larger than about 0.46, that is, about half its maximum value, we find $d-d_0>0$. For the calculation of δ according to Eq. (3), the experimental bulk values for the interlayer spacing $d_0=2.86$ Å and the Fermi wavelength $\lambda_F=3.66$ Å (Ref. 42) were taken.

C. Influence of the substrate: Effects of strain

Although the oscillations in d with the slab thickness are undoubtedly recovered from the *ab initio* results and supported by the simple concept of a misfit, the difference between theory and experiment with respect to the sign of $d-d_0$ (the 1 ML phase shift discussed in Sec. IV B) remains puzzling.

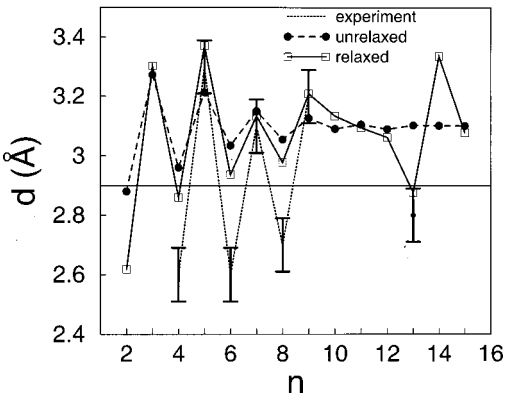

FIG. 7. Calculated apparent step heights for compressed slabs $\overline{\rho_0}=1\times10^{-4}$ electrons/Å^3, for relaxed and unrelaxed geometries, compared to experimental values (Ref. 23).

There are quite a few reasons, both from theory and experiment as to why this discrepancy might occur. Here we concentrate on possible errors introduced by the neglect of the Cu(111) substrate. The substrate will influence both the geometry and the electronic structure of the Pb film. Here we focus on the former. Because Cu and Pb have different lattice constants, the Pb overlayers are compressed in the surface plane with respect to bulk Pb, in particular for layers close to the substrate. From previous LEED studies on this system[36] it is known that Pb on Cu(111) arranges in a $p(4\times4)$ pattern, which leads to a $\sim$2.6% in-plane compression in the first layer of the Pb film due to the different lattice constants for Pb and Cu. More recent LEED studies[43] have reported that after the completion of the first Pb monolayer the layers deposited on Cu(111) are more strained than in the commensurate $p(4\times4)$ phase, being 3.3% compressed at 1.2 ML of coverage, and are still under 1.1% compression at 5 ML.

To account for this substantial intra-plane strain, we performed calculations where the in-plane lattice constant was compressed by 3.3%. In other words, the supercell dimensions in the surface plane were reduced by 3.3%. No additional constraints were imposed on the system geometry. Reducing the supercell dimensions imposes the same compression on all layers. This treatment is of course only approximate but the main trends due to the geometric constraints imposed by a Cu(111) substrate should become obvious. With such an in-plane compression the notion of an unrelaxed geometry is somewhat arbitrary: we chose to make the unit cell volumes of the compressed and uncompressed systems equal for a given n, and to expand the the interlayer spacings and the vacuum gap accordingly.

In Fig. 7 the apparent step heights with the intralayer compression are shown and compared to experiment. Results for both relaxed and unrelaxed geometries are shown. The step heights were calculated for a density of $\overline{\rho}=1\times10^{-4}$ electrons/Å^3. There are several interesting points to note.

First, the experimental and the theoretical apparent step heights are now ''in phase'', i.e., maxima and minima of d appear at the same n.

Second, the quantitative agreement between experiment and theory worsens as n increases. This is easy to understand since the in-plane compression reduces in the real system with increasing n while in our simple model the compression remains the same.

Third, the theoretical curves appear to be shifted upward relative to experiment. This may be because we have only accounted for the geometric influence of the substrate. The in-plane compression will ''squeeze'' the electron density into the vacuum and increase the spill-out. It is possible that the change in electronic potential due to the Cu substrate would counter this effect. Again, over compression exaggerates the problem at large n.

Despite these differences in detail, it is clear that the lateral compression is an excellent candidate to explain remaining quantitative differences between theory and experiment. As a corollary, the major influence exerted on the Pb films by their Cu substrate is in-plane compression.

V. SUMMARY AND CONCLUSIONS

In summary, quantum size effects in thin lead films epitaxially grown on a Cu(111) substrate have been investigated with gradient-corrected periodic density functional calculations. QSE-related oscillations—often with a double-layer period—in the total energies and in the ''apparent step heights'' have been detected, both of which have been measured by HAS experiments by Toennies and co-workers.[22,23] Good semiquantitative agreement between theory and experiment was found, in particular when interplane relaxation and in-plane strain imposed by the substrate was accounted for.

The major conclusions are as follows.

(1) The *ab initio* calculations confirm qualitatively the jellium calculations by Schulte,[7] for a ''real'' system.

(2) However, the existence of real ionic cores rather than a diffuse, positive jellium background is important when a more quantitative treatment is required. This is most evident from comparing unrelaxed with relaxed calculations. While the oscillations in total energies are somewhat insensitive to the actual positions of the ion cores, the ''geometric'' contribution to the apparent step heights is typically of the same order of magnitude as the ''electronic'' effects and cannot be neglected.

(3) In-plane strain imparted by the Cu substrate appears to have a significant effect on the apparent step heights. It must be taken into account to yield the correct location of maxima and minima in the calculated apparent step heights. When the effect of strain is accounted for, the agreement between calculated and experimental data is very satisfactory.

(4) As a methodological point we note that the accurate determination by DFT of electron spillouts far from the film is a challenge, both for fundamental (the form of the exchange-correlation functional) and practical reasons (size of the vacuum gap).

In effect the oscillations in the charge density outside the film reflect oscillations in the work function, as is obvious from Eq. (9). Therefore we expect that work function measurements on thin lead films would indicate QSE-related oscillations as well.[10] This is to be expected also for other metal films or clusters and it is an important issue as the work function, for example, directly relates to the chemical and catalytic activity of a system.

Of course, the present theoretical treatment can be improved in several ways. For the electronic structure part the explicit inclusion of the Cu(111) substrate would be highly desirable, and would also allow the determination of the appropriate interfacial geometry. The details of this geometry are bound to be important given our findings concerning in-plane strain. As far as the modelling of HAS is concerned a more realistic He-film potential should be determined and the He scattering process treated quantum mechanically.

In any case the Cu(111)/Pb(111) system is an excellent candidate for carrying out this type of calculation in the future, largely because of the ongoing experimental interest in this system as a ''microlab'' for the study of quantum size effects in metallic nanostructures.[44,45]

ACKNOWLEDGMENTS

Fruitful discussion with G.F. Tantardini (Milan) are gratefully acknowledged. We thank the United-Kingdom Car-Parrinello Consortium (UKCP) for a generous allocation of time on the CSAR National facilities. The CASTEP code was made available to UCL through the UKCP-MSI Agreement, 1999.

[1] V. B. Sandomirskii, Zh. Eksp. Teor. Fiz. **52**, 158 (1967) [Sov. Phys. JETP **25**, 101 (1967)].

[2] W. D. Knight, K. Clemenger, W. A. de Heer, W. A. Saunders, M. Y. Chou, and M. L. Cohen, Phys. Rev. Lett. **52**, 2141 (1984); V. Aviyente, I. Baccarelli, B. Balta, F. A. Gianturco, and C. Selcuki, in *Quantum Systems in Physics and Chemistry*, edited by R. McWeeny and R. Wilson (1998).

[3] K.-J. Jin, G. D. Mahan, H. Metiu, and Z. Zhang, Phys. Rev. Lett. **80**, 1026 (1998).

[4] H. Brune, C. Romainczyk, H. Roder, and K. Kern, Nature (London) **369**, 469 (1994).

[5] H. Roder, E. Hahn, H. Brune, J.-P. Bucher, and K. Kern, Nature (London) **366**, 141 (1993); J. M. Garcia, O. Sanchez, P. Segovia, J. E. Ortega, J. Alvarez, A. L. V. de Parga, and R. Miranda, Appl. Phys. A: Mater. Sci. Process. **61**, 609 (1995).

[6] M. I. Elinson, V. A. Volkov, V. N. Lutskij, and T. N. Pinsker, Thin Solid Films **12**, 383 (1972).

[7] F. K. Schulte, Surf. Sci. **55**, 427 (1976).

[8] P. J. Feibelman and D. R. Hamann, Phys. Rev. B **29**, 6463 (1984).

[9] A. Kiejna, J. Peisert, and P. Schraroch, Surf. Sci. **432**, 54 (1999).

[10] J. C. Boettger and S. B. Trickey, Phys. Rev. B **45**, 1363 (1992);

U. Birkenheuer, J. C. Boettger, and N. Rösch, Chem. Phys. Lett. **341**, 103 (1995); K. F. Wojciechowski and H. Bogdanów, Surf. Sci. **397**, 53 (1998); K. Doll, N. M. Harrison, and V. R. Saunders, J. Phys.: Condens. Matter **11**, 5007 (1999).
[11] P. Saalfrank, Surf. Sci. **274**, 449 (1992).
[12] R. C. Jaklevic, J. Lambe, M. Mikkor, and W. C. Vassell, Phys. Rev. Lett. **26**, 88 (1971); R. C. Jaklevic and J. Lambe, Phys. Rev. B **12**, 4146 (1975).
[13] B. T. Jonker, N. C. Bartelt, and R. L. Park, Surf. Sci. **127**, 183 (1983); B. T. Jonker and R. L. Park, *ibid.* **146**, 93 (1984); **146**, 511 (1984); Solid State Commun. **51**, 871 (1984); H. Iwasaki, B. T. Jonker, and R. L. Park, Phys. Rev. B **32**, 643 (1985).
[14] M. Jałochowski and E. Bauer, Phys. Rev. B **38**, 5272 (1988).
[15] M. Jałochowski, M. Hoffman, and E. Bauer, Phys. Rev. Lett. **76**, 4227 (1996).
[16] B. G. Orr, H. M. Jaeger, and A. M. Goldman, Phys. Rev. Lett. **53**, 2046 (1984).
[17] S. S. Parkin, Phys. Rev. Lett. **67**, 3598 (1991); P. Grünberg, R. Schreiber, Y. Pang, M. D. Brodsky, and H. Sowers, *ibid.* **57**, 2442 (1986); J. Unguris, R. J. Celotta, and D. T. Pierce, *ibid.* **67**, 140 (1991).
[18] J. E. Ortega, F. J. Himpsel, G. J. Mankey, and R. F. Willis, Phys. Rev. B **47**, 1540 (1993).
[19] R. Kläsges, D. Shmitz, C. Carbone, W. Eberhardt, P. Lang, R. Zeller, and P. H. Dederichs, Phys. Rev. B **57**, R696 (1998).
[20] R. H. Brown, D. M. C. Nicholson, W. H. Butler, X.-G. Zhang, W. A. Shelton, T. C. Schulthess, and J. M. MacLaren, J. Appl. Phys. **81**, 4008 (1997).
[21] For a review on magnetic nanostructured systems see F. J. Himpsel, J. E. Ortega, G. J. Mankey, and R. F. Willis, Adv. Phys. **47**, 511 (1998); F. J. Himpsel, J. Phys.: Condens. Matter **11**, 9483 (1999).
[22] B. J. Hinch, C. Koziol, J. P. Toennies, and G. Zhang, Europhys. Lett. **10**, 341 (1989); B. J. Hinch, C. Koziol, J. P. Toennies, and G. Zhang, Vacuum **42**, 309 (1991).
[23] J. Braun and J. P. Toennies, Surf. Sci. **384**, L858 (1997).
[24] Y. S. Li, F. Jona, and P. M. Marcus, Phys. Rev. B **43**, 6337 (1991).
[25] M. C. Payne, M. P. Teter, D. C. Allan, T. A. Arias, and J. D. Joannopoulos, Rev. Mod. Phys. **64**, 1045 (1992).
[26] W. Kohn and L. J. Sham, Phys. Rev. **140**, 1133A (1965).
[27] J. P. Perdew and Y. Wang, Phys. Rev. B **45**, 13 244 (1992).
[28] D. Vanderbilt, Phys. Rev. B **41**, 7892 (1990).
[29] D. D. Koelling and B. N. Harmon, J. Phys. C **10**, 3107 (1977).
[30] G. B. Bachelet and M. Schluter, Phys. Rev. B **25**, 2103 (1982); L. Kleinman, *ibid.* **21**, 2630 (1980).
[31] M. J. Gillan, J. Phys.: Condens. Matter **1**, 689 (1989).
[32] G. Kresse and J. Furthmüller, Phys. Rev. B **54**, 11 169 (1996).
[33] W. H. Press, S. A. Teukolsky, W. T. Vetterling, and B. P. Flannery, *Numerical Recipes (in FORTRAN): The Art of Scientific Computing*, 2nd ed. (Cambridge University Press, Cambridge, 1992), Chap. 10.
[34] N. D. Mermin, Phys. Rev. **137**, A1441 (1965).
[35] H. J. Monkhorst and J. D. Pack, Phys. Rev. B **13**, 5188 (1973).
[36] J. Henrion and G. E. Rhead, Surf. Sci. **29**, 20 (1972).
[37] K. Horn, B. Reihl, A. Zartner, D. E. Eastman, K. Hermann, and J. Noffke, Phys. Rev. B **30**, 1711 (1984).
[38] M. Methfessel, D. Hennig, and M. Scheffler, Phys. Rev. B **46**, 4816 (1991).
[39] N. Esbjerg and J. K. Nǿrskov, Phys. Rev. Lett. **45**, 807 (1980).
[40] S. Heinze, S. Blügel, R. Pascal, M. Bode, and R. Wiesendanger, Phys. Rev. B **58**, 16 432 (1998); G. Hörmandinger, *ibid.* **49**, 13 897 (1994).
[41] W. H. Green Jr., D. J. Tozer, and N. C. Handy, Chem. Phys. Lett. **290**, 465 (1998).
[42] J. R. Anderson and A. V. Gould, Phys. Rev. **139**, A1459 (1965).
[43] G. Meyer, M. Michailov, and M. Henzler, Surf. Sci. **202**, 125 (1988).
[44] R. Otero, A. L. V. de Parga, and R. Miranda, Surf. Sci. **447**, 143 (2000).
[45] S. Müller, J. E. Prieto, C. Rath, L. Hammer, R. Miranda, and K. Heinz, Appl. Phys. Lett. (to be published).